Spectrochimica Acta Part A 76 (2010) 395–400

Contents lists available at ScienceDirect

Spectrochimica Acta Part A: Molecular and Biomolecular Spectroscopy

journal homepage: www.elsevier.com/locate/saa

The structure of betaxolol studied by infrared spectroscopy and natural bond orbital theory

João Canotilho*, Ricardo A.E. Castro

Center for Pharmaceutical Studies, Faculty of Pharmacy, University of Coimbra, Pólo das Ciências da Saúde, Azinhaga de Santa Comba, Coimbra 3000-548, Portugal

ARTICLE INFO

Article history:
Received 7 January 2010
Received in revised form 24 March 2010
Accepted 29 March 2010

Keywords:
Betaxolol
β-Blocker
Infrared spectroscopy
Natural bond orbital (NBO) analysis
Density functional theory

ABSTRACT

Betaxolol is a selective β_1 receptor blocker used in the treatment of hypertension and glaucoma. A study of the betaxolol structure based on infrared spectroscopy and natural bond orbital (NBO) theory is the main aim of the present research.

FTIR spectra of the solid betaxolol were recorded in the region from 4000 to 400 cm^{-1}, in the temperature range between 25 and −170 °C. For spectral interpretation, spectrum of the deuterated betaxolol and the theoretical vibrational spectra of the conformer present in the solid obtained at the B3LYP/6-31G* level of theory, were used. Further insight into the structure was provided by natural bond orbital theory. NBO analysis of the conformer, before and after optimization, was carried out at the same level of theory referred above.

Vibrational modes involved in hydrogen bond in the stretching and bending region were used in the estimation of the enthalpy using empirical correlations between enthalpy and the frequency shift that occurs as a result of the establishment of intermolecular hydrogen bonds.

A detailed study of the structure of betaxolol and of its intermolecular interactions was obtained from the combination spectroscopy and NBO theory.

1. Introduction

This paper deals with the study of the structure of betaxolol (1-[4-[2-(cyclopropylmethoxy)ethyl]phenoxy]-3-(1-methylethylamino)propan-2-ol) carried out by infrared spectroscopy. This compound is used as β-adrenergic antagonist in cardiovascular diseases and glaucoma treatment [1]. The structure of most β-blockers consists of an aryloxypropanoamine and a molecular group attached to the aromatic ring. The β-blockers of this type differ one from another by the aromatic and the substituent group. The structure and the atom labelling are given in Fig. 1.

The interpretation of spectra in the solid state needs a reference spectrum of the compound under consideration. This spectrum is a valuable aid to identify the vibration bands and is also used to evaluate the influence of the intermolecular forces on the structure. The reference is commonly the experimental spectra of the isolated molecule either obtained by experimental via (inert solvent, vapor phase, matrix-isolation) or calculated by conformer analysis. Both practical and theoretical procedures are difficult applied to a compound like betaxolol due to its molecular dimensions, low solubility and volatility. Thus our reference spectrum is that of the optimized structure of the isolated molecule with the conformation present in the solid state. Such reference has the advantage to correspond to a structure close to that of the solid state under consideration [2,3]. The structure of the solid was performed by the authors [4] and the X-ray diffraction data are available in Cambridge Crystallographic Data Centre (CCDC No. 648386).

The effect of the temperature on the spectra pattern, deuteration and natural bond analysis supports the interpretation of the spectroscopic results.

2. Materials and methods

(*R*,*S*)-Betaxolol was obtained from alkaline solutions of very pure (>99.9%) betaxolol hydrochloride by solvent extraction. The organic phase was evaporated, the resulting solid dissolved in methanol:water (20:80 percent, v/v) cosolvent and crystallized by very slow evaporation of the solvent at room temperature. The solid thus obtained was used in the spectroscopic experiments.

The spectra of solid betaxolol dispersed into a potassium bromide pellet were recorded in a Thermo Nicolet IR 300 spectrometer. Sixteen scans, with resolution of 1 cm^{-1}, were run for each spectrum. The spectra obtained were analysed using EZOmnic program [5].

* Corresponding author at: Center for Pharmaceutical Studies, Faculty of Pharmacy, University of Coimbra, Portugal.
E-mail addresses: jcano@ci.uc.pt (J. Canotilho), rcastro@ff.uc.pt (R.A.E. Castro).

1386-1425/$ – see front matter © 2010 Elsevier B.V. All rights reserved.
doi:10.1016/j.saa.2010.03.038

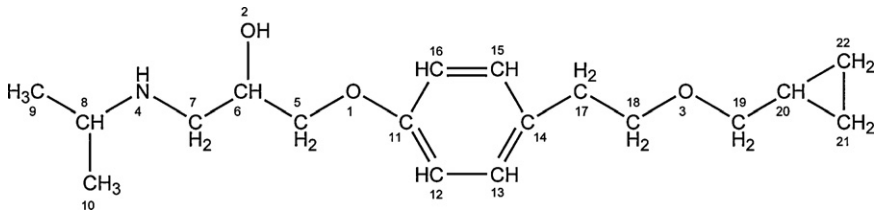

Fig. 1. Betaxolol molecular structure and atom numbering.

Spectra were recorded at temperature between −170 and 25 °C. A cell with calcium fluoride windows and a temperature control device supplied by Graseby Specac were used to record these. To avoid water vapor condensation on the cell walls at low temperatures the cell compartment was kept under vacuum by Edwards High Vacuum equipment consisting of a two-stage rotary pump in association with a turbomolecular pump. The temperature variation inside the cell was approximately ±0.5 °C.

To obtain the deuterated betaxolol solid samples were maintained in equilibrium with methanol-d (CH_3OD) (99.5 atom%) at 40 °C for 1 h under argon atmosphere. The liquid was then removed by evaporation at reduced pressure.

3. Theoretical vibration spectra

The vibrational spectrum was obtained by full optimization of the molecular structure given by X-ray diffraction. The calculation was performed at B3LYP/6-31G(d,p) level of theory, using Gaussian03 computational chemistry package [6]. No imaginary frequencies were found. The calculated vibrational frequencies were scaled by the recommended factor of 0.9613 [7].

An approximated band assignment was performed by GaussView [8]. Table 1 contains the wavenumbers and intensities for the spectra from 4000 to 400 cm^{-1}. Spectra of the optimized structure changing OH and NH by OD and ND were also calculated.

4. Infrared spectra of the betaxolol

The experimental spectra of betaxolol at 25 °C between 4000 and 2000 cm^{-1} and of the partially deuterated compound are depicted in Fig. 2(a). In Fig. 2(b) is traced the calculated spectra from the optimized structure of the isolated molecule with the conformation present in the solid state of betaxolol and the corresponding deuterated one.

As expected, one can observe the stretching vibration of the OH, NH and CH groups. By deuteration, the absorption bands localized in 3600–3100 cm^{-1} region move to 2500–2000 cm^{-1}, a manifestation of deuterable groups (Fig. 3). By fitting the spectrum of the solid betaxolol at 25 °C in that region using Lorentzian functions three component bands were found with $\bar{\nu}_{max}$ at 3372, 3279 and 3138 cm^{-1}. The first band is a very weak of increasing wavenumber as the temperature decreases and is vanished by deuteration. Apparently it is an overtone or combination band of the NH group. The second band corresponds to the stretch vibration mode of N4—H and the last one is the O2—H stretch vibration mode. These bands present a frequency isotopic ratio of 1.35 and 1.38, respectively, in good agreement with theoretical expectations. The influence of the temperature on the infrared spectra can be used to evidence hydrogen bonds since with the decreasing of the temperature the hydrogen bonds gets stronger [9,10]. In betaxolol, the frequency of the stretching bands N4—H and O2—H decreases from 25 to −170 °C, 3 and 9 cm^{-1}, respectively.

Considering to the wavenumbers of the free groups given by the optimized free molecule, the establishment of the N—H···O and O—H···N hydrogen bonds gives rise to a redshift of 94 and 542 cm^{-1}, respectively. Several empirical equations relate $\Delta\nu$ and ΔH of the hydrogen bond; $(\Delta H)^2 = 1.92[(\Delta\nu) - 40]$ [11]; $\Delta H = -(75.24\Delta\nu)/(720 + \Delta\nu)$ [12]. The values estimated for ΔH using both equations gives similar values, 10 or 9 kJ mol^{-1} (N—H···O) and 31 or 32 kJ mol^{-1} (O—H···N), respectively. The hydrogen bond N—H as donor is much weaker than that as acceptor.

The existence of intermolecular hydrogen bond is also evidenced by NBO carried out with the NBO 5.0 program [13]. Fig. 4 shows overlap of ligand and antiligand orbitals, n(NH) → σ*(O) and n(OH) → σ*(N), on two adjacent betaxolol molecules, removed from the crystalline network of betaxolol [4] and obtained by single point at B3LYP/6-31G(d,p) level of theory.

It is clear that n(OH) → σ*(N) overlap is much higher than that of n(NH) → σ*(O) overlap. It is also observable the linearity of the

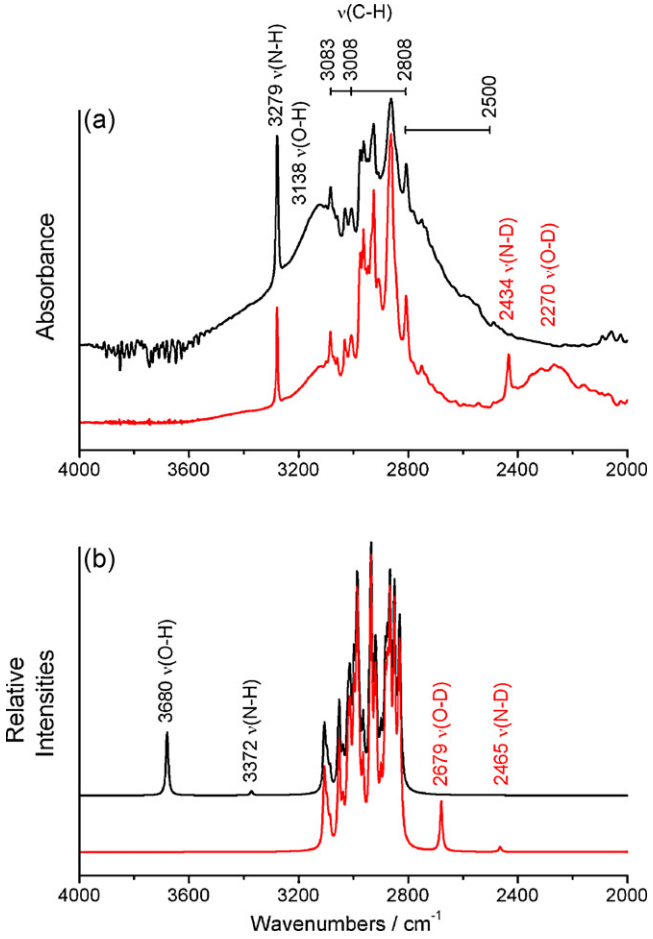

Fig. 2. Betaxolol infrared spectra in 4000–2000 cm^{-1} region: (a) experimental (black line – without deuteration, red line – partially deuterated) and (b) calculated (black line – for the isolated molecule, red line – for the isolated molecule deuterated). (For interpretation of the references to colour in this figure legend, the reader is referred to the web version of the article.)

Table 1
Calculated wavenumbers (cm^{-1}), calculated IR intensities (I), and approximate description for betaxolol.

ν (cm^{-1})	I_{cal} ($km\,mol^{-1}$)	Approximate description
3680	24.9	ν(O2—H)
3372	1.7	ν(N4—H)
3106	25.1	ν_a(C21—H_2), ν_a(C22—H_2) i.p.
3096	11.1	ν(C16—H)
3092	0.9	ν_a(C21—H_2), ν_a(C22—H_2) o.p.
3085	6.9	ν(C12—H)
3053	17.9	ν(C13—H)
3051	16.2	ν(C15—H)
3038	10.9	ν(C20—H)
3022	12.7	ν_s(C21—H_2), ν_s(C22—H_2) i.p.
3017	22.0	ν_s(C21—H_2), ν_s(C22—H_2) o.p.
3012	28.2	ν_a(C10—H_3)
2998	39.5	ν_a(C9—H_3)
2987	71.0	ν_a(C9—H_3), ν_a(C10—H_3) i.p.
2979	19.3	ν_a(C17—H_2)
2978	3.0	ν_a(C9—H_3), ν_a(C10—H_3) o.p.
2964	22.3	ν_a(C7—H_2)
2936	63.1	ν_a(C5—H_2)
2935	29.2	ν_s(C17—H_2)
2921	35.4	ν_s(C9—H_3), ν_s(C10—H_3) i.p.
2917	11.3	ν(C6—H)
2915	15.8	ν_s(C9—H_3), ν_s(C10—H_3) o.p.
2899	16.3	ν(C8—H)
2884	40.7	ν_s(C5—H_2)
2876	36.0	ν_s(C18—H_2)
2866	68.8	ν_a(C19—H_2)
2850	71.3	ν_s(C18—H_2), ν_s(C19—H_2) i.p.
2835	22.3	ν_s(C18—H_2), ν_s(C19—H_2) o.p.
2830	52.7	ν_s(C7—H_2)
1608	64.4	ν(C=C) ring
1568	12.2	ν(C=C) ring
1500	134.2	δ(C—H) ring
1486	0.9	δ(C18—H_2), δ(C19—H_2) i.p.
1471	4.3	δ(C18—H_2), δ(C19—H_2) o.p., δ(C—H) Δ i.p.
1467	48.6	δ(C5—H_2), δ(C7—H_2)
1466	29.0	δ(C5—H_2), δ(C9—H_3), δ(C10—H_3) i.p.
1463	6.9	δ(C9—H_3), δ(C10—H_3) i.p., δ(N4—H)
1463	8.3	δ(C19—H_2)
1458	2.4	δ(C7—H_2)
1449	2.0	δ(C17—H_2)
1443	2.6	δ(C9—H_3), δ(C10—H_3) o.p.
1441	2.0	δ(C9—H_3), δ(C10—H_3) o.p.
1430	22.0	δ(N4—H)
1427	1.1	δ(C21—H_2), δ(C22—H_2) o.p.
1411	8.7	w(C18—H_2), w(C19—H_2) o.p.
1407	1.2	δ(C—C—H) ring in plane
1398	16.8	δ(C6—H), δ(O2—H)
1374	8.5	δ(C9—H_3), δ(C10—H_3) i.p. umbrella
1372	5.3	w(C5—H_2), w(C7—H_2)
1364	36.0	w(C17—H_2), w(C18—H_2) o.p.
1356	10.6	δ(C9—H_3), δ(C10—H_3) o.p. umbrella
1337	6.8	δ(O2—H), w(C7—H_2), δ(C8—H)
1322	40.2	w(C18—H_2), w(C19—H_2) i.p., δ(C20—H)
1312	14.1	δ(C8—H), δ(N4—H), δ(C6—H)
1309	39.0	δ(C8—H), tw(C17—H_2)
1304	13.0	δ(C8—H)
1297	20.8	δ(C5—H), δ(C6—H), δ(C7—H)
1289	9.8	δ(C—H) ring in plane i.p.
1271	7.3	w(C17—H_2), w(C18—H_2) i.p.
1259	8.0	tw(C17—H_2), tw(C18—H_2) i.p.
1255	30.1	δ(O2—H), δ(C6—H), δ(C7—H)
1239	360.7	ν(C11—O1)
1237	8.8	tw(C19—H_2)
1202	22.7	δ(O2—H), δ(C6—H), tw(C7—H_2), δ(N4—H) oop
1191	18.0	tw(C5—H_2)
1185	2.8	tw(C17—H_2), tw(C18—H_2) i.p.
1183	1.0	ν(C—C) Δ breathing
1182	0.2	tw(C17—H_2), tw(C18—H_2) o.p.
1159	17.2	δ(C—H) ring in plane o.p.
1156	6.3	tw(C—H) Δ, tw(C19—H_2)
1154	62.8	ν(C8—N1)
1154	1.6	tw(C—H) Δ, tw(C19—H_2)
1140	22.0	δ(O2—H), δ(C6—H), tw(C7—H_2), δ(N4—H) in plane
1108	294.5	ν(C18—O3), ν(C19—O3)
1106	50.9	ν(C7—N4), ν(C4—C5)
1100	13.6	δ(C—H) ring in plane o.p.
1092	67.1	tw(C—H) Δ
1090	18.6	ν(C7—N4), ν(C8—C9)
1078	24.0	ν(C5—C6)
1064	61.4	ν(C6—O2), δ(O2—H), ρ(C1—H_2)
1051	5.3	ν(C17—C18)
1039	33.6	ν(C5—C6), ν(C6—O2), ρ(C7—H_2)
1037	5.7	w(C21—H_2), w(C22—H_2) i.p.
1036	105.9	ν(C5—O1)
1023	3.9	w(C21—H_2), w(C22—H_2) o.p.
1015	7.0	tw(C17—H_2), ρ(C18—H_2)
998	6.7	ν(C17—C18)
991	0.7	δ(CCC) ring
984	20.2	ρ(C19—H2), ν(C19—C20), ν(C21—C22)
928	8.6	ν(C8—N4), ρ(C9—H_3) ρ(C10—H_3) i.p.
925	0.1	δ(C—H) ring oop
917	11.2	ρ(C19—H_2), ρ(C—H_2) Δ
913	1.0	ρ(C9—H_3) ρ(C10—H_3) o.p.
909	0.3	δ(C—H) ring oop
894	4.4	ρ(C5—H_2), ρ(C7—H_2)
894	4.3	ρ(C9—H_3) ρ(C10—H_3) o.p.
890	7.1	ν(C—C) Δ
866	9.1	ν(C6—C7), ρ(C5—H_2)
832	12.0	⌀ ring breathing
816	5.7	ν(C—C) Δ, δ(C—H) ring oop
812	16.1	ν(C—C) Δ, δ(C—H) ring oop
809	29.4	ν(C8—C9), ν(C8—C10), δ(N4—H)
794	9.2	δ(C—H) ring oop
789	4.3	ρ(C—H_2) Δ
776	0.3	ρ(C17—H_2), ρ(C18—H_2)
766	2.4	ν(C14—C17), δ(N4—H)
754	69.1	δ(N4—H) oop
749	2.5	ρ(C—H) Δ
703	1.8	⌀ ring flipping chair
629	0.8	δ(C—C—C) ring in plane
583	17.4	δ(C5—O1—C11), δ(C—C—C) ring, δ(C14—C17—C18)
537	10.9	δ(C—H) ring oop, δ(C5—O1—C11)
514	3.6	δ(C—H) ring oop
492	11.7	ρ(C7—H_2)
482	7.7	δ(C7—N4—C8), δ(C5—C6—C7)
457	0.7	δ(O3—C19—C20)
428	3.8	δ(C18—O3—C19)
426	1.5	δ(N4—C8—C9), δ(N1—C8—C10)
409	0.6	δ(C—H) ring oop
405	5.3	δ(C8—C9—C10), ρ(C7—H_2)
369	1.3	δ(C19—C20—C21), δ(C19—C20—C22)

Abbreviations: a, antisymmetric; s, symmetric; ν, stretching; δ, in plane deformation; w, wagging; ρ, rocking; tw, twisting; τ, torsion; i.p., in-phase; o.p., out-of-phase; oop, out-of-plane deformation.

intermolecular hydrogen bond in the n(OH) → σ*(N) overlap. This is in agreement with the ΔH results found for both bonds.

The C—H stretching vibration bands are in 3083–2808 cm^{-1}, Fig. 2. This interval can be considered as subdivided into two: one between 3083 and 3008 cm^{-1} correspond to the stretch vibration of the C—H aromatic and cyclopropyl rings and the other 3008–2808 cm^{-1} to the saturated aliphatic CH groups.

The former region is presented in Fig. 5. By comparison to the calculated spectra three distinct vibrational regions can be assigned in the experimental spectra: the first corresponds to the in-phase antisymmetric stretch vibration ν_a(C21—H_2) + ν_a(C22—H_2); the second to the C—H aromatic stretch vibrations; the third to the symmetric stretch vibration ν_s(C21—H_2) + ν_s(C22—H_2).

The phenyl and cyclopropyl groups of betaxolol play an important role in the structural point of view [4]. The pharmacological activity results from the interaction of phenyl, hydroxyl and amino groups with the binding sites of the β-adrenoreceptor. The antagonist activity results from the molecular complementarity [14]. The

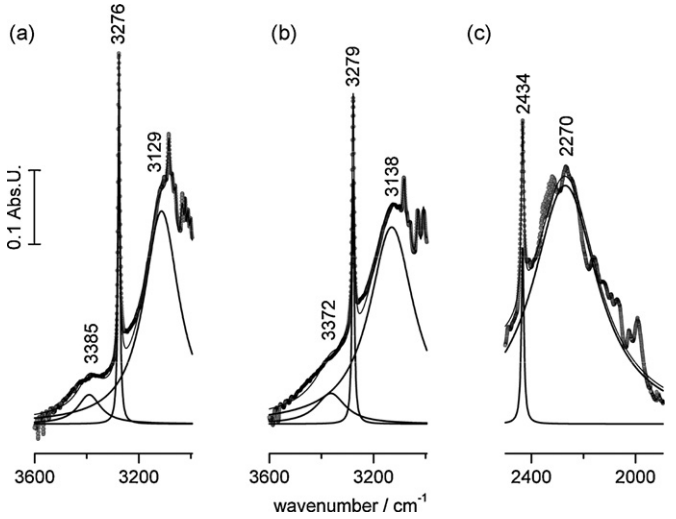

Fig. 3. The deconvoluted infrared spectra of: (a) betaxolol at −170 °C; (b) betaxolol at 25 °C; and (c) partially deuterated betaxolol at 25 °C.

cyclopropyl group, due to the reactivity resulting from the high strain is part of many reagents [15–18] and also of a large number of active pharmaceutical ingredients [19–21]. Thus this spectral region deserves particular attention. The infrared spectroscopic data are accompanied by NBO. In order to evaluate the effect of the intermolecular forces the hybrid conformation C—H bonds single point of the isolated molecule with the conformations in the solid and this structure optimized at level of theory referred before.

The electron delocalization in the phenyl ring is extended to O1 atoms. The hybrid in C—O bond is sp. It is observed the overlap of the electron lone-pair orbital of this atom with vicinal antiligand orbitals the strongest is the LP2O1 (p character) with the antiligand C11═C12 orbital. The energy corresponding to this interaction is 123.72 kJ mol^{-1}.

Unlike C—C bonds the carbon hybridization in C—H of the phenoxyl and cyclopropyl groups are similar. The s richer character of the C—H hybrid in C—C relatively to the tetrahedric hybridization of the aliphatic C—H explains the higher frequency of the stretch vibration. In both groups the optimization leads to a slight decrease of the s-character of the band, Table 2.

Most organic compounds have many C—H bonds which result in medium intensity bands. The band discrimination corresponding to the stretch vibration of the aliphatic CH bonds in 3008–2808 cm^{-1} would be difficult to succeed in. It would not be worthy because not much information could be obtained from this effort.

Table 2
Hybridization type of the carbon atoms of the C—H bonds in the phenoxyl and cyclopropyl groups (SP – single point; Opt. – optimized).

Bond	Phenoxyl group		Bond	Cyclopropyl group	
	SP	Opt.		SP	Opt.
C12—H37	$sp^{2.02}$	$sp^{2.34}$	C20—H47	$sp^{2.15}$	$sp^{2.67}$
C13—H38	$sp^{2.16}$	$sp^{2.44}$	C21—H48	$sp^{2.16}$	$sp^{2.55}$
C15—H39	$sp^{2.18}$	$sp^{2.45}$	C21—H49	$sp^{2.25}$	$sp^{2.52}$
C16—H40	$sp^{2.04}$	$sp^{2.34}$	C22—H50	$sp^{2.37}$	$sp^{2.53}$
			C22—H51	$sp^{2.45}$	$sp^{2.55}$

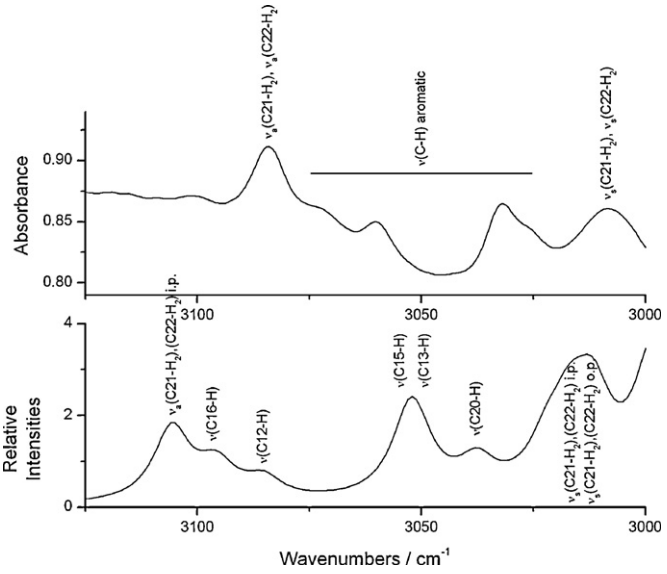

Fig. 5. Betaxolol CH stretch 3125–3000 cm^{-1} region: up – experimental at 25 °C; down – calculated for the isolated molecule.

Strong absorption is observed in the spectra of the solid state in 2808–2500 cm^{-1}. The calculated spectra and that of deuterated solid betaxolol show less absorption in this region what leads to the conclusion that the bands are due to non-fundamental vibration modes. Absorption in this spectral region was observed in previous works published by authors on molecules similar to that of betaxolol [2,3,22].

The 1700–1000 cm^{-1} wavenumber range contains bands arising from the C—H in plane bending modes as well as stretch of C—C, C—O, C—N. Although a detailed analysis of the spectra in this region becomes difficult, since a heavy band overlap occurs, a tentative

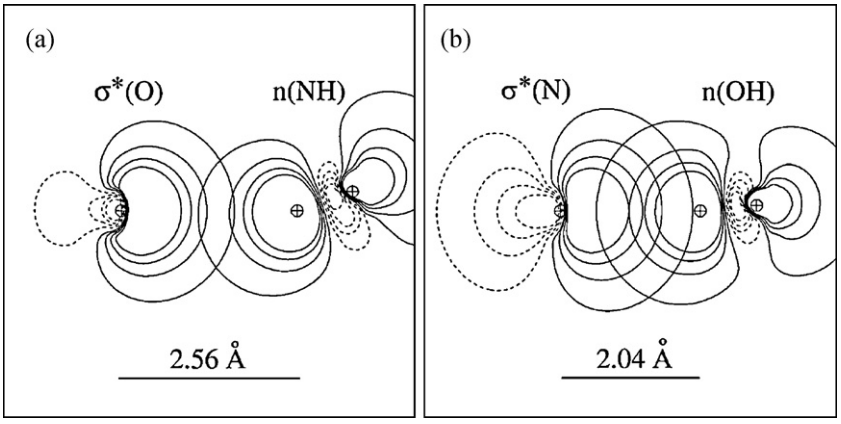

Fig. 4. NBO 2D contours of the intermolecular hydrogen bond: (a) n(NH) → σ*(O) and (b) n(OH) → σ*(N). Heavy atoms distances are shown in the picture.

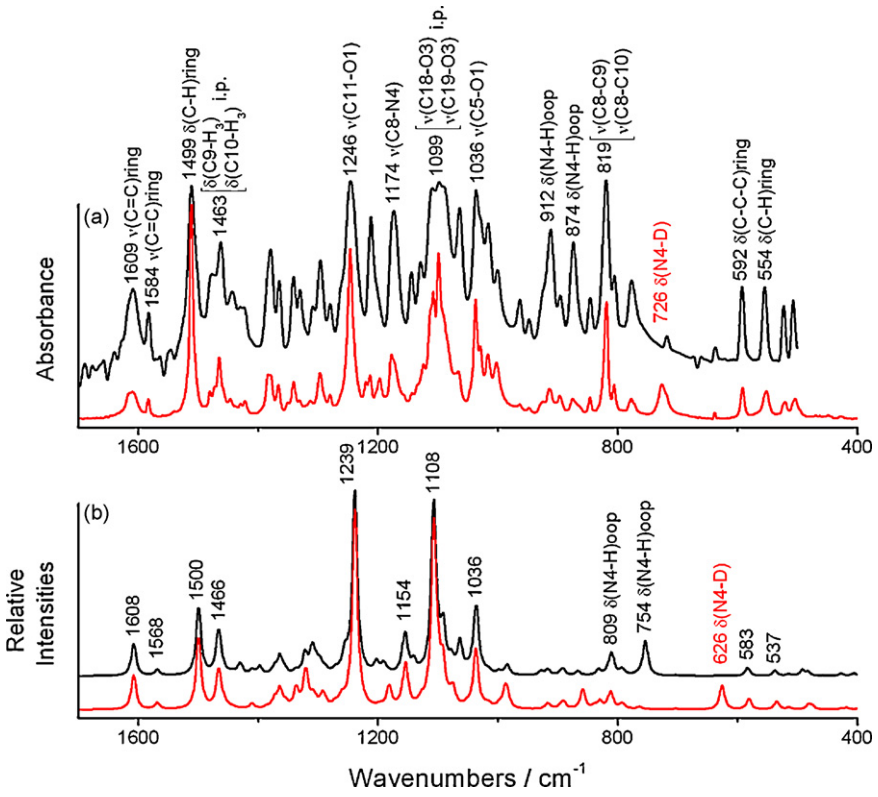

Fig. 6. Betaxolol infrared spectra in 1700–400 cm^{-1} region: (a) experimental (black line – without deuteration, red line – partially deuterated) and (b) calculated (black line – for the isolated molecule, red line – for the isolated molecule deuterated). (For interpretation of the references to colour in this figure legend, the reader is referred to the web version of the article.)

Table 3
NBO composition of the O—C bond.

Bond	Ether groups	
	SP	Opt.
O1—C5	$0.8256(sp^{2.63})_{O1} + 0.5642(sp^{4.37})_{C5}$	$0.8264(sp^{2.43})_{O1} + 0.5631(sp^{3.93})_{C5}$
O1—C11	$0.8222(sp^{2.03})_{O1} + 0.5692(sp^{3.05})_{C11}$	$0.8228(sp^{2.03})_{O1} + 0.5683(sp^{3.03})_{C11}$
O3—C18	$0.8172(sp^{2.60})_{O3} + 0.5764(sp^{4.00})_{C18}$	$0.8205(sp^{2.55})_{O3} + 0.5717(sp^{3.70})_{C18}$
O3—C19	$0.8168(sp^{3.09})_{O3} + 0.5770(sp^{4.26})_{C19}$	$0.8202(sp^{2.57})_{O3} + 0.5721(sp^{3.77})_{C19}$

assignment of various bands and ν_{max} are indicated in the spectra, Fig. 6.

A manifestation of structural features can be observed in the nature of the two ether groups present in the molecule. In fact, ν(C11—O1) = 1246 cm^{-1}, ν(C18—O3) and ν(C19—O3) = 1099 cm^{-1} while ν(C5—O1) = 1036 cm^{-1}.

In Table 3 it is evident that hybrid of O1 in O1—C11 has the more pronounced s-character justifying the higher wavenumber value. This electron delocalization promoted by phenyl ring is also responsible by the C5—O1 wavenumber position.

In Fig. 6, the 1000–400 cm^{-1} region presents the out-of-plane bending vibration modes of the N4—H. The involvement of the NH group in intermolecular hydrogen bonding gives rise to a blue shift and enhancement of the bands. In fact, in the calculated spectra these vibration modes gives rise to two bands with ν_{max} 809 and 754 cm^{-1} that are shifted in the experimental spectra to 912 and 874 cm^{-1}, respectively. By partial deuteration these bands almost disappear and it is evidence the out-of-plane bending of N4—D at 726 cm^{-1}. The blue shift in this region is also used to calculate the strength of hydrogen bond, $(-\Delta H = 0.67 \times 10^{-4} \times [(\nu_H)^2 - (\nu_0)^2])$ [23]. The energy involved is 12 and 13 kJ mol^{-1}, respectively, figure in agreement with that estimated from the NH shift for the stretching vibration mode.

5. Conclusions

Infrared spectroscopy provides relevant information on structure and intermolecular interactions in betaxolol. The vibrational spectrum calculated, for the conformation obtained from X-ray diffraction data, is used as reference spectrum in order to quantify the intermolecular hydrogen bonds. NBO theory provides an excellent approach to interpret the infrared spectra in electronic terms. Relative band positions, together with displacement of bands corresponding to molecular groups not involved in hydrogen bonds, are explained by this theory.

Acknowledgment

The authors are grateful to FEDER/POCI 2010 for financial support.

References

[1] B.B. Hoffman, in: J.G. Hardman, L.E. Limbird, A.G. Gilman (Eds.), The Pharmacological Basis of Therapeutics, 10th ed., McGraw-Hill, New York, 2001, p. 215.

[2] R.A.E. de Castro, J. Canotilho, R.M. Barbosa, J.S. Redinha, Spectrochim. Acta, Part A 67 (2007) 1194.
[3] R.A.E. Castro, J. Canotilho, S.C.C. Nunes, M.E.S. Eusebio, J.S. Redinha, Spectrochim. Acta, Part A 72 (2009) 819.
[4] J. Canotilho, R.A.E. Castro, M.T.S. Rosado, M. Ramos Silva, A. Matos Beja, J.A. Paixão, J. Simões Redinha, J. Mol. Struct. 891 (2008) 437.
[5] OMNIC 6.1a, Thermo Nicolet Corporation, 2001.
[6] M.J. Frisch, G.W. Trucks, H.B. Schlegel, G.E. Scuseria, M.A. Robb, J.R. Cheeseman, J.J.A. Montgomery, T. Vreven, K.N. Kudin, J.C. Burant, J.M. Millam, S.S. Iyengar, J. Tomasi, V. Barone, B. Mennucci, M. Cossi, G. Scalmani, N. Rega, G.A. Petersson, H. Nakatsuji, M. Hada, M. Ehara, K. Toyota, R. Fukuda, J. Hasegawa, M. Ishida, T. Nakajima, Y. Honda, O. Kitao, H. Nakai, M. Klene, X. Li, J.E. Knox, H.P. Hratchian, J.B. Cross, V. Bakken, C. Adamo, J. Jaramillo, R. Gomperts, R.E. Stratmann, O. Yazyev, A.J. Austin, R. Cammi, C. Pomelli, J.W. Ochterski, P.Y. Ayala, K. Morokuma, G.A. Voth, P. Salvador, J.J. Dannenberg, V.G. Zakrzewski, S. Dapprich, A.D. Daniels, M.C. Strain, O. Farkas, D.K. Malick, A.D. Rabuck, K. Raghavachari, J.B. Foresman, J.V. Ortiz, Q. Cui, A.G. Baboul, S. Clifford, J. Cioslowski, B.B. Stefanov, G. Liu, A. Liashenko, P. Piskorz, I. Komaromi, R.L. Martin, D.J. Fox, T. Keith, M.A. Al-Laham, C.Y. Peng, A. Nanayakkara, M. Challacombe, P.M.W. Gill, B. Johnson, W. Chen, M.W. Wong, C. Gonzalez, J.A. Pople, Gaussian 03, Revision D. 01, Gaussian, Inc, Wallingford, CT, 2004.
[7] J.B. Foresman, Frish Exploring Chemistry with Electronic Structure Methods, 2nd ed., Gaussian, Inc, Pittsburgh, PA, 1996.
[8] R. Dennington II, T. Keith, J. Millam, GaussView, Version 4.1.2, Semichem, Inc, Shawnee Mission, KS, 2007.
[9] H.O. Desseyn, S.P. Perlepes, K. Clou, N. Blaton, B.J. Van der Veken, R. Dommisse, P.E. Hansen, J. Phys. Chem. A 108 (2004) 5175.
[10] H.O. Desseyn, K. Clou, R. Keuleers, R. Miao, V.E. Van Doren, N. Blaton, Spectrochim. Acta, Part A 57 (2001) 231.
[11] A.V. logansen, Spectrochim. Acta, Part A 55 (1999) 1585.
[12] A.A. Stolov, M.D. Borisover, B.N. Solomonov, J. Phys. Org. Chem. 9 (1996) 241.
[13] E.D. Glendening, J.K. Badenhoop, A.E. Reed, J.E. Carpenter, J.A. Bohmann, C.M. Morales, F. Weinhold, NBO 5.0, Theoretical Chemistry Institute, University of Wisconsin, Madison, 2001.
[14] R.B. Silverman, The Organic Chemistry of Drug Design and Drug Action, 2nd ed., Elsevier Academic Press, San Diego, 2004 (Chapter 3).
[15] C.J. Suckling, Angew. Chem., Int. Ed. Engl. 27 (1988) 537.
[16] P.B.M.W.M. Timmermans, in: R. Dahlbom, J.G.L. Nillsson (Eds.), Medicinal Chemistry, Swedish Pharmaceutical Press, Stockholm, 1985, p. 69.
[17] L. Colombo, Tetrahedron Lett. 36 (1995) 625.
[18] A.D. Headley, Bioorg. Chem. 31 (2003) 99.
[19] C. Cativiela, Tetrahedron 53 (1997) 4479.
[20] C. Craig, K. Christine, Thrombin Inhibitors, A61K31/4985; A61K31/551; A61P7/02 ed., 1998.
[21] A.P. Ayala, H.W. Siesler, S. Wardell, N. Boechat, V. Dabbene, S.L. Cuffini, J. Mol. Struct. 828 (2007) 201.
[22] J. Edler, P. Hamm, Phys. Rev. B: Condens. Matter. 69 (2004) 214301.
[23] M.S. Rozenberg, Spectrochim. Acta, Part A 52 (1996) 1559.